ISSS Journal of Micro and Smart Systems (2021) 10:41–50
https://doi.org/10.1007/s41683-021-00068-3

ORIGINAL ARTICLE

Design, analysis and fabrication of 4H–SiC diaphragm for piezoresistive MEMS pressure sensor

Mahesh Kumar Patankar[1] · Aparna Gupta[2] · M. Kasinathan[1] · R. P. Behera[1] · T. Jayanthi[1] · Nandita DasGupta[2] · Sandip Dhara[3]

Received: 3 September 2020 / Revised: 10 February 2021 / Accepted: 16 April 2021 / Published online: 15 May 2021
© Institute of Smart Structures & Systems, Department of Aerospace Engineering, Indian Institute of Science, Bangalore 2021

Abstract

A diaphragm-based MEMS pressure sensor, suitable for harsh environments, was designed, simulated, analyzed and virtually fabricated on *p*-type SiC epitaxial semi-insulating 4H–SiC substrate to measure the external pressure in the range of 0–8 MPa using device simulation software. The critical component of the pressure sensor is a thin flat square SiC diaphragm with an area of 1500 μm × 1500 μm and thickness of 75 μm. The area and thickness were optimized by performing computer simulation using the finite element method of simulation. The *p*-type SiC resistors were virtually fabricated in Wheatstone bridge configuration on top of the SiC diaphragm to convert the mechanical stress signal, generated due to external pressure into an electrical output voltage signal. The 4H–SiC MEMS pressure sensor was virtually fabricated on high-purity semi-insulating SiC substrate by dry etching method and its sensitivity was obtained at 2.42 μV/V/KPa for the operating pressure range. A thin SiC diaphragm was fabricated toward the realization of the SiC piezoresistive MEMS pressure sensor.

Keywords MEMS · Piezoresistive · SiC diaphragm · HPSI · Plasma etching

Introduction

Conventional Si-based pressure sensors cannot perform at a temperature greater than 150 °C due to unacceptably high leakage current in the *p–n* junction. The operating temperature can be extended up to 250 °C using Si on insulator (SOI) technology. However, beyond 500 °C, the thermal deformation of Si diaphragm imposes the ultimate limiting factor (Wijesundara and Azevedo 2011). SiC is a promising material for application in the harsh environments because of its excellent chemical stability, wide band gap, as well as higher breakdown voltage, thermal conductivity, electron mobility and radiation resistance as compared to those for Si (Lebedev et al. 2004). In consideration of the above factors, SiC is used as a material to measure the unknown pressure in piezoresistive micro-electromechanical systems (MEMS) pressure sensor configuration.

For realizing the high-temperature and radiation-resistant MEMS sensors, the structural stability of the material is extremely important. The exciting feature of SiC is its appearance in many different polytypes. The most common polytypes of SiC for developing the MEMS structures and electronics are 3C, 4H and 6H (Zettterling 2002). These polytypes of SiC also exhibit excellent piezoresistive effect (Wijesundara and Azevedo 2011; Nguyen et al. 2018; Shore et al. 1993) and are compatible with microfabrication technologies. Among them, 4H-SiC offers higher mobility along the *c*-axis (Zettterling 2002), isotropic piezoresistance in (0001) plane (Nguyen et al. 2018) and is commercially available in wafer form with upto 150 mm diameter. Many researchers studied SiC pressure sensors having 3C–SiC piezoresistors on Si or SiO_2/Si diaphragms (Wu et al. 2001; Zappe et al. 2001; Eickhoffa et al.

✉ Mahesh Kumar Patankar
patankar@igcar.gov.in

1 Real Time Systems Division, Indira Gandhi Centre for Atomic Research, Homi Bhabha National Institute, Kalpakkam, Tamil Nadu 603102, India

2 Electrical Engineering Department, Indian Institute of Technology Madras, Chennai, Tamil Nadu 600 036, India

3 Surface and Nanoscience Division, Indira Gandhi Centre for Atomic Research, Homi Bhabha National Institute, Kalpakkam, Tamil Nadu 603102, India

1999).Okojie et al. (1998) fabricated the 6H–SiC pressure sensor using circular diaphragm on *n*-type 6H–SiC substrate. For similar work, Okojie et al. (2015) demonstrated the piezoresistive sensor fabricated using *n*-type epitaxial layer as piezoresistor on the 4° off-axis basal (0001)-plane (Si-face) of a semi-insulating 4H–SiC substrate to minimize the leakage current as compared to the piezoresistors fabricated on the SiC conductive substrate. Akiyama et al. (2011) also realized the *n*-type 4H–SiC pressure sensor using circular diaphragm on SiC conductive substrate.

In the present work, a square diaphragm-based piezoresistive 4H–SiC MEMS pressure sensor is designed, analyzed and virtually fabricated on *p*-type SiC epitaxial high-purity semi-insulating (HPSI) SiC substrate for the measurement of pressure in harsh environments. The pressure-sensitive square SiC diaphragm is realized on the semi-insulating substrate by performing the bulk micromachining with an area of 1500 μm × 1500 μm and thickness of 75 μm considering space restriction for future application. Piezoresistor structure was virtually fabricated using *p*-type SiC epitaxial layer to measure the target pressure of 8 MPa. As a novelty, *p*-SiC-type piezoresistors on square SiC diaphragm are reported by using the semi-insulating SiC substrate in this paper. In addition, fabrication of SiC diaphragm with the desired dimension using plasma etching to realize SiC piezoresistive pressure sensor is demonstrated.

Pressure sensing mechanism

Different kinds of pressure sensing mechanisms are possible. Among them, piezoresistive, capacitive (Stephen Ming-Chang Hou 2003) and piezoelectric (NajafiSohi 2013) are popular sensing techniques. The piezoelectric effect is more suitable for dynamic pressure measurement whereas, the capacitive effect results in more nonlinearity and also requires more fabrication steps than those for the piezoelectric effect. The piezoresistive effect can be used for the measurement of static and dynamic pressure as well, and at the same time, it requires fewer fabrication steps. Semiconductor material offers high strain gauge factor as compared to metal and can be fabricated using conventional lithography techniques in the microelectronics industry.

Sensor design criteria

The diaphragm-based pressure sensor is simple in design and requires few fabrication steps. The key elements of 4H-SiC MEMS pressure sensor are thin elastic SiC diaphragm and *p*-type piezoresistors. The diaphragm experiences the mechanical stress in the presence of external pressure and piezoresistors, located on top of it, change their resistivity due to the applied stress, which in turn translates into an electrical voltage signal.

Diaphragm design considerations

There are different possible geometries of the diaphragm. The commonly used geometries are square, rectangle and circular. Among them, square geometry is more suitable for MEMS pressure sensor because it produces the maximum stresses and therefore, the maximum output can be generated over diaphragms of other geometries with the same plane area (Hsu 2008). In addition, from the sensor fabrication point of view, it is easy to dice the square diaphragm from the standard SiC wafers. Thus, for designing a 4H-SiC MEMS pressure sensor, a square-shaped diaphragm was preferred.

To find out the mechanical response of SiC thin diaphragm, load–deflection method was adopted. In this technique, deflection of a suspended film is measured as a function of applied pressure. The load–deflection relation of a flat square diaphragm clamped at all four sides is given by the following equation (Mario 1982):

$$\frac{Pa^4}{Yh^4} = \frac{66.2}{(1-v^2)}\left(\frac{y}{h}\right) + \frac{31.1}{(1-v^2)}\left(\frac{y}{h}\right)^3 \tag{1}$$

where P is applied pressure, Y is Young's modulus, v Poisson's ratio of the diaphragm material, a is the side length of the diaphragm, h is the diaphragm thickness and y is the center deflection of the diaphragm. According to the load–deflection method, the deflection range is divided into two regions, namely a small deflection region (deflection less than 25% of the diaphragm thickness) described by the linear term in Eq. (1), and a large deflection region (deflection greater than 25% of the diaphragm thickness) described by the nonlinear, cubic term in Eq. (2). To design the sensor and maintain the linearity between applied pressure and stress, it is obvious that the diaphragm must deflect at the center and the deflection must be less than the quarter thickness of the diaphragm. Thus, to understand the mechanical performance of the square diaphragm, the first term of Eq. (1) given below is considered under the uniform load:

$$y = \frac{Pa^4(1-v^2)}{66.2Yh^3} \tag{2}$$

The second crucial factor which greatly affects the performance of the diaphragm is stress generation in the presence of external pressure. The maximum stress $\sigma_{\max}$ occurring in the middle of the diaphragm edges is given by the following equation (Mario 1982):

$$\sigma_{\max} = 0.3078 \frac{Pa^2}{h^2} \tag{3}$$

In a square diaphragm, due to the symmetry of the structure, stress components in xx and yy direction are equal and can be calculated by the following equation:

$$(\sigma_{xx})_{\max} = (\sigma_{yy})_{\max} = 0.3078 \frac{Pa^2}{h^2} \tag{4}$$

where σ_{xx} and σ_{yy} are mechanical stresses in xx and yy directions, respectively. For designing the square SiC diaphragm, Young's modulus = 500 GPa, Poisson ratio = 0.2 and material density = 3.3 g/cm^3 were considered. The side length of the square diaphragm was optimized at 1500 µm, whereas its thickness was taken as 75 µm to measure the pressure in 0–8 MPa range considering the various requirements for future application including space and pressure range.

Design of SiC resistors

The next important component of 4H–SiC MEMS pressure sensor is the p-type SiC resistors. To detect the change in pressure, the piezoresistivity effect in a semiconductor is considered. When a material is stretched or compressed its resistivity changes. This phenomenon is called piezoresistivity and this is significantly larger for semiconductors than that for metals (Sawhney 1995). The electrical resistance (R) in a homogeneous structure depends on its dimensions and resistivity (ρ) and is mathematically defined as the following relation (Barlian et al. 2009):

$$R = \frac{\rho L}{A} \tag{5}$$

where L is the length and A is the cross-sectional area of the structure. It is clear from Eq. (5) that under the influence of applied stress, the dimensions of the structure and its resistivity change, resulting in the change of the resistance. To quantify the piezoresistive effect, the term Gauge factor G is commonly used and it varies from material to material. The Gauge factor is expressed as the fractional change in the resistance per unit strain (Barlian et al. 2009):

$$G = \frac{\Delta R}{R \cdot \varepsilon} = (1 + 2v) + \frac{\Delta \rho}{\rho \cdot \varepsilon} \tag{6}$$

where $\varepsilon = \Delta L / L$ is the strain. For the practical purpose, the geometrical changes are often not considered in the case of piezoresistive materials since the piezoresistive effect is dominant. Thus, the gauge factor in the semiconducting material is given by the following equation:

$$G = \frac{\Delta R / R}{\varepsilon} = \frac{\Delta \rho / \rho}{\varepsilon} \tag{7}$$

The relative change in resistivity is greatly influenced by the applied stress and can also be presented as a function of the applied stress (σ) and piezoresistive coefficient (π) as

$$\frac{\Delta \rho}{\rho} = \pi \cdot \sigma \tag{8}$$

The change in electrical resistance ΔR due to longitudinal stress π_l and transverse stress π_t can be expressed as follows (Stephen Ming-Chang Hou 2003):

$$\frac{\Delta R}{R} = \pi_l \sigma_l + \pi_t \sigma_t \tag{9}$$

To convert the mechanical stress generated in SiC diaphragm due to external uniform pressure, into an electrical voltage signal, four p-type SiC resistors are formed in the specified zone of the SiC diaphragm and connected in Wheatstone bridge configuration. The details of the basic pressure sensor structure are given in the schematic diagram shown in Fig. 1. The physical dimensions for SiC diaphragm and p-type SiC resistors are shown in Table 1.

The resistor arrangement on the front side of the SiC diaphragm is shown in Fig. 2. As already mentioned, SiC piezoresistors are configured as a Wheatstone bridge. The electrical output voltage proportional to the pressure can be represented using the following equation:

$$V_o = \frac{0.3078}{2} (\pi_l - \pi_t)(1 - \upsilon) \cdot \left(\frac{a}{h}\right)^2 \cdot P \cdot V_s \tag{10}$$

where V_o denotes to the electrical output voltage, V_s is the supply voltage for the operation of the pressure sensor. The Wheatstone bridge is one of the most sensitive and precise methods for detecting small changes in resistance. Any change in the piezoresistance due to externally applied pressure causes the bridge output voltage to change. An essential advantage of the Wheatstone bridge configuration is that if the bridge is perfectly balanced under the condition when $R_1 = R_2 = R_3 = R_4$, a small change in the resistance can be detected and measured. Besides this, a change in temperature will affect all the resistors equally. Thus, even if the resistance changes with temperature, the change is equal for all the resistors and the bridge is still balanced perfectly.

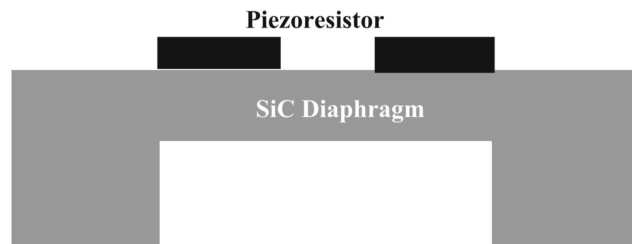

Fig. 1 4H-SiC MEMS pressure sensor structure

Table 1 Design parameters for SiC pressure sensor

Component	Mechanical dimension in μm	Thickness in μm
Thin SiC Diaphragm	1500 × 1500	75
Piezoresistors	10 (W) × 400 (L)	1

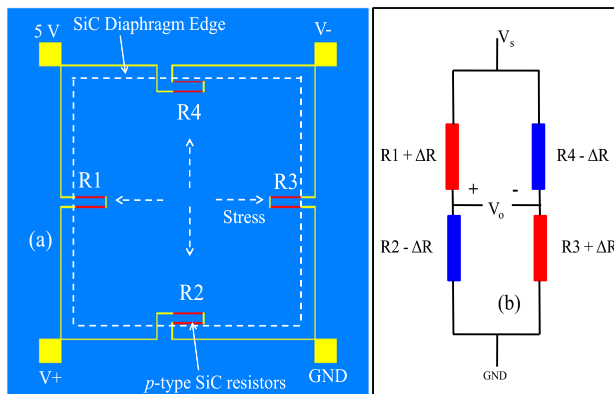

Fig. 2 A bridge constructed using four p-type SiC resistors. **a** Piezoresistors arrangement on top side of the SiC diaphragm **b** Wheatstone bridge configuration

Pressure sensor simulation

The pressure sensor simulation work was carried out in two phases using device simulation software. To understand the mechanical stress distribution on SiC diaphragm due to external pressure, FEM simulation work was executed independently. Thereafter, the electrical response of pressure sensor due to mechanical stress generated in the diaphragm-resistors assembly, composed of SiC diaphragm and piezoresistors, was simulated and analyzed by varying the operating pressure.

FEM simulation

To optimize the square size of the SiC diaphragm for the entire pressure range, FEM simulation was performed using device simulation software. Figure 3a shows the *xx*-component of stress (952 MPa) generated in SiC diaphragm in the longitudinal direction due to external pressure at full load, whereas Fig. 3b represents the *yy*-component of stress distribution profile over the surface of the SiC diaphragm in the transverse direction at the full load. Figure 3c shows the Von mises stress distribution profile over the surface of the diaphragm. It shows that the four maximum stress regions of equal magnitude are located at the center of the diaphragm edges. Understanding the stress distribution profile across the entire surface of the diaphragm is very important to determine the placement of the piezoresistors.

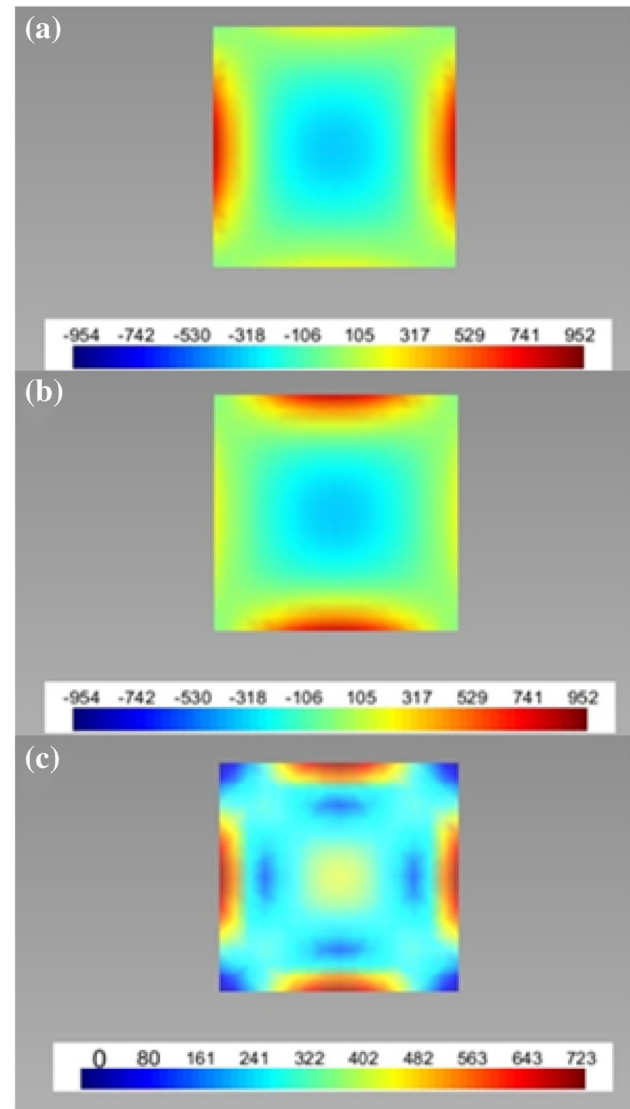

Fig. 3 Stress distribution profile due to external pressure at full load. **a** Sxx component of stress: 952 MPa **b** Syy component of stress: 952 MPa **c** Von mises stress profile

Figure 4 shows the mechanical stress components, i.e. *Sxx* and *Syy*, in the longitudinal direction and the same components at transverse direction as well due to square shape geometry. The stress difference between the stress components (*Sxx* and *Syy* in the longitudinal direction) is significantly less as shown in Fig. 4 with a flat line around the central zone of the diaphragm and maximum value along the central edges of the diaphragm, and Fig. 4 also indicates that the piezoresistors can be placed along the

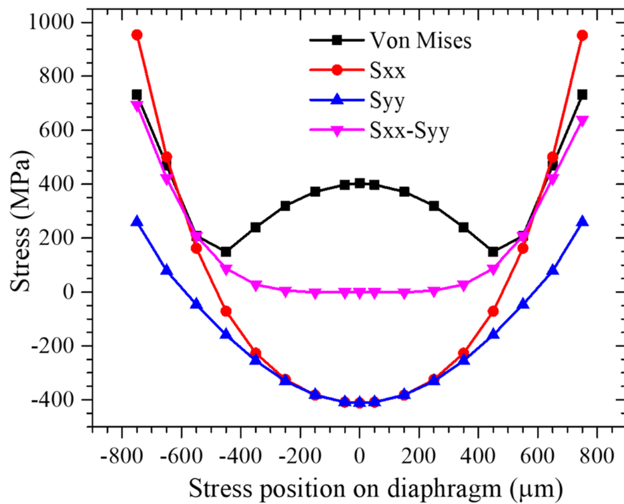

Fig. 4 Stress components profile in the longitudinal direction under the influence of pressure at full load

center of the edges. Thus, it is decided to place the piezoresistors along the center of the edges in the split form where diaphragm offers maximum stress which is very much essential to change the resistance of all the resistors equally. The other important information is the deflection of the diaphragm due to the applied pressure.

Figure 5 shows the distribution of deflection on the SiC diaphragm at full load which is significantly less as compared to the thickness of the diaphragm to assist in obtaining the linear output voltage due to linearly varying pressure. The maximum deflection is 2.85 μm as compared to the thickness of the diaphragm. Figure 6 shows the plot for the diaphragm displacement along the central line generated with respect to maximum operating pressure for the pressure sensor.

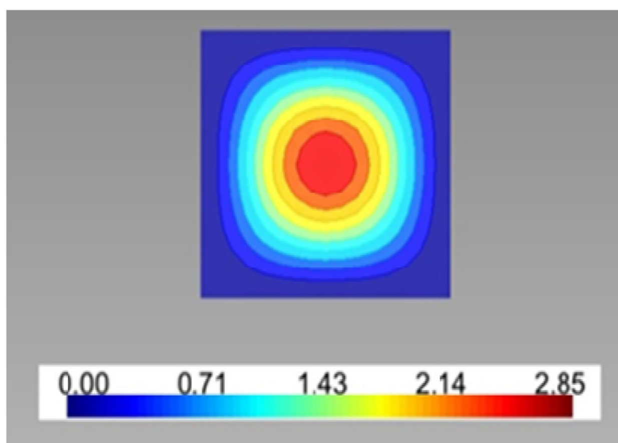

Fig. 5 Diaphragm displacement distribution profile in μm under the influence of external pressure at full load

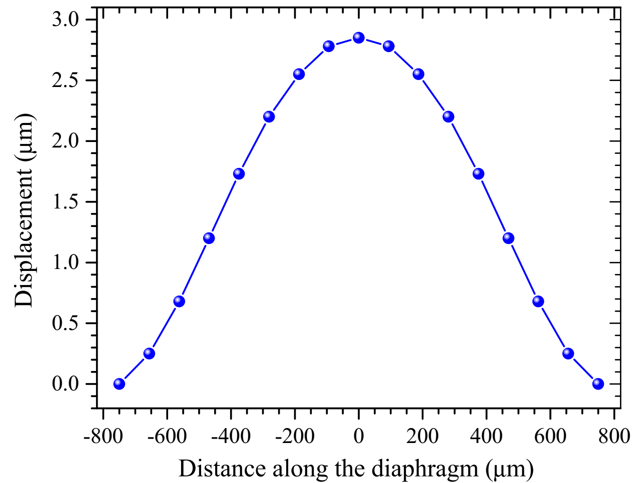

Fig. 6 Diaphragm displacement profile along the central line under the influence of pressure at full load

Piezoresistive simulation

To translate the mechanical stresses generated in SiC diaphragm due to uniform applied pressure into a measurable electrical output voltage signal, the sensing elements (*p*-type piezoresistors) were considered at maximum stress zone on the front side of the diaphragm. Each *p*-type piezoresistor value was considered at 2 KΩ, and all piezoresistors were interconnected in Wheatstone bridge configuration. To execute the piezoresistive simulation, the fundamental piezoresistive coefficients: π_{11}, π_{12}, and π_{44} which denote the longitudinal, transverse and shear piezoresistive coefficients, respectively, were used (Nguyen et al. 2018).

$$\pi_{11} = 6.43 \times 10^{-5} 1/\text{MPa}$$

$$\pi_{12} = -5.12 \times 10^{-5} 1/\text{MPa}$$

$$\pi_{44} = 0$$

The pressure sensor assembly is drawn using device simulation software to execute the piezoresistive simulation and analysis purpose. Initially, boundary conditions of the diaphragm are defined, and subsequently, material properties of the diaphragm and piezoresistors are specified as considered in mathematical computations. After performing all the settings, the electrical simulation was executed, and the corresponding change in the output voltage due to pressure for 0–8 MPa range was obtained at room temperature. To execute the piezoresistive simulation, + 5 V_{dc} was applied to the Wheatstone bridge circuit and change in the output voltage due to uniform pressure up to 8 MPa was obtained. The pressure sensor assembly including piezoresistors under the influence of uniform pressure at full load is shown in Fig. 7. It is clear that all the piezoresistors experience the maximum stress at the middle

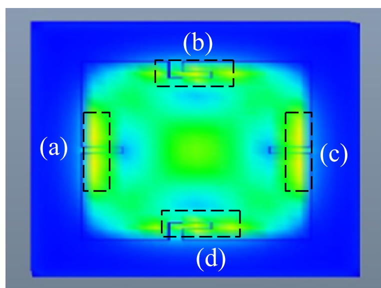

Fig. 7 Maximum stress zone on SiC diaphragm denoted by dotted blocks **a–d** for piezoresistors placement on SiC diaphragm

edge of the diaphragm as annotated by dotted blocks (Fig. 7).

Virtual fabrication of pressure sensor

The 4H-SiC MEMS pressure sensor was realized through virtual fabrication route using device simulation software. The virtual fabrication details of the proposed SiC pressure sensor are summarized as follows: A *p*-type SiC epitaxial layer on HPSI SiC substrate with a resistivity of ≥ 1E5 Ω-cm and thickness of 350 μm was chosen as the substrate for the realization of the SiC pressure sensor. For creating the piezoresistors, the first photolithography was performed on the *p*-type SiC epitaxial layer of the semi-insulating substrate. The reactive ion etching method was performed to pattern the piezoresistors. A 500-nm-thick SiO_2 layer was deposited using plasma-enhanced chemical vapor deposition on the front side of the substrate. In SiO_2 layer openings were created using the second photolithography. Thereafter, thin Ti/Au was deposited and patterned by defining third photolithography for making the electrical connection between the piezoresistors in Wheatstone bridge configuration and metal pads. In the next step, bulk micromachining was performed backside of the substrate to create a 75-μm-thick SiC diaphragm. The photoresist was applied to the backside of the substrate and patterned using fourth photolithography.

To initiate the backside etching, Ni, a hard mask material, was deposited on the backside by electroplating and lift-off process was used to remove the photoresist. Later, SiC diaphragm was created by the inductively coupled plasma reactive ion etching (ICP-RIE*)* method. Finally, Ni was etched completely from the backside. Finally, the bonding between SiC substrate and AIN substrate was executed as a part of wafer bonding and a through-hole was etched in AIN for applying pressure to the pressure sensor. The main steps in the fabrication process are illustrated in schematic Fig. 8.

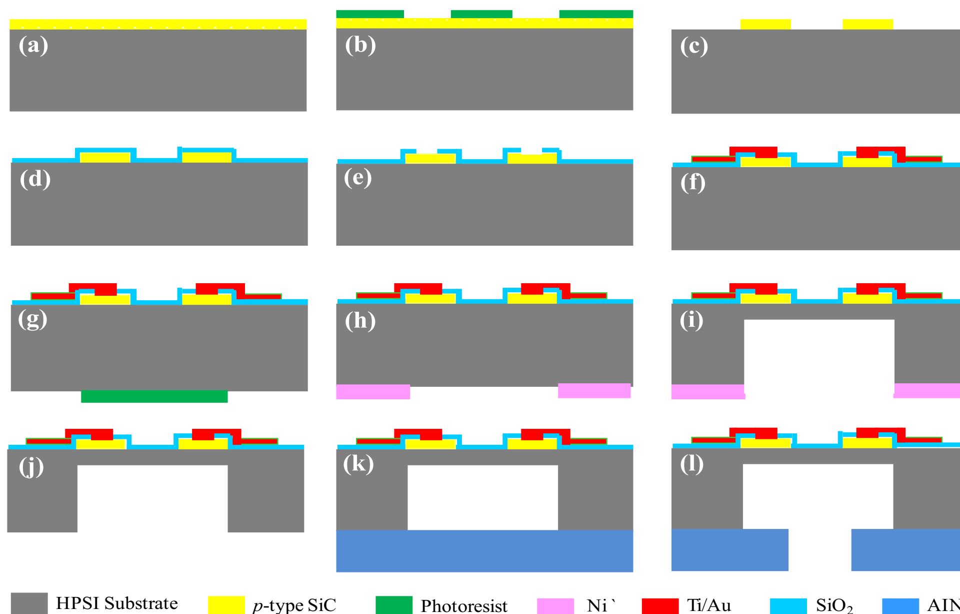

Fig. 8 Major fabrication steps for the proposed 4H-SiC MEMS pressure sensor: **a** p-type 4H-SiC epitaxial HPSI SiC Substrate **b** Photoresist patterned by the first photolithography **c** Piezoresistor structure created by p-type 4H-SiC epitaxial etching **d** Deposition of SiO_2 isolation layer **e** The Ohmic contact holes patterned by the second photolithography **f** Ti/Au deposited and patterned by the third photolithography **g** Photoresist patterned by the fourth photolithography **h** Nickel electroplating **i** SiC diaphragm creation using ICP-RIE method **j** Nickel Etching **k** Bonding between HPSI substrate and AIN substrate **l** Through-hole AIN etching for creating the pressure port

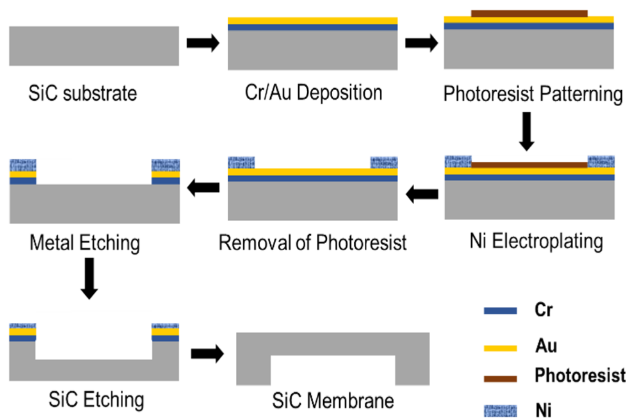

Fig. 9 Process flow for fabrication of SiC diaphragm

Fabrication of SiC diaphragm

As mentioned in the preceding section, SiC square diaphragm with a thickness of 75 µm is required for the designed pressure sensor. The major challenge in fabrication of SiC diaphragm is the selective etching of SiC with controlled etch rate and dimensions to realize the diaphragm structure (Zettterling 2002; Mehregany et al. 1998; Tanaka et al. 2001). Due to the high bond energy between Si and C, there is no chemical etchant for SiC at room temperature. Naturally, a plasma-based dry etching method has been considered as an efficient route for SiC etching. However, the choice of mask materials to withstand SiC etching condition is limited.

Double-side polished SiC wafers (4H and 6H) with a thickness of 350 µm were taken as the starting material. After a standard cleaning process, blanket etching of SiC was performed to thin down the wafer. Since the wafer thickness is 350 µm, it is difficult to perform selective etching of SiC to obtain the desired diaphragm thickness of 75 µm. In order to solve this problem, blanket etching was adopted prior to selective etching. Blanket etching of SiC substrate was carried out using a gas mixture of O_2 and SF_6 in ICP-RIE to achieve the final thickness $\sim$ 175–200 µm. The etching process was optimized by varying process parameters such as flow rates of SF_6 and O_2, pressure, ICP and RF power, temperature and time. In order to realize the SiC diaphragm with a final thickness $\sim$ 75 µm, it is necessary to etch selective portions of the bulk from the backside using Ni as the mask material, which has been widely used as a mask for selective etching of SiC (selectivity $\sim$ 20–70) (Dowling et al. 2017). In order to etch around 120 µm of SiC, it is required to deposit at least 8–10 µm of Ni to act as an effective mask during the etching process. Electroplating method was adopted to deposit thick Ni using patterned Cr/Au (thickness $\sim$ 20 nm/120 nm) as a seed layer. Ni was electroplated using a Watt's bath recipe and pulsed current with a current density of 8–12 mA/cm^2 for 40–60 min of growth to obtain 8–10-µm thick layer. Following Ni electroplating process, the unmasked layer of Cr/Au (not protected by nickel) was etched to create the window for SiC etching. Finally, SiC was selectively etched using O_2 and SF_6 in ICP-RIE, maintaining the optimized flow rate of SF_6 and O_2 as 50 sccm and 10 sccm, respectively to attain the final SiC diaphragm of thickness $\sim$ 75 µm. The entire process flow of fabrication of SiC diaphragm is shown Fig. 9.

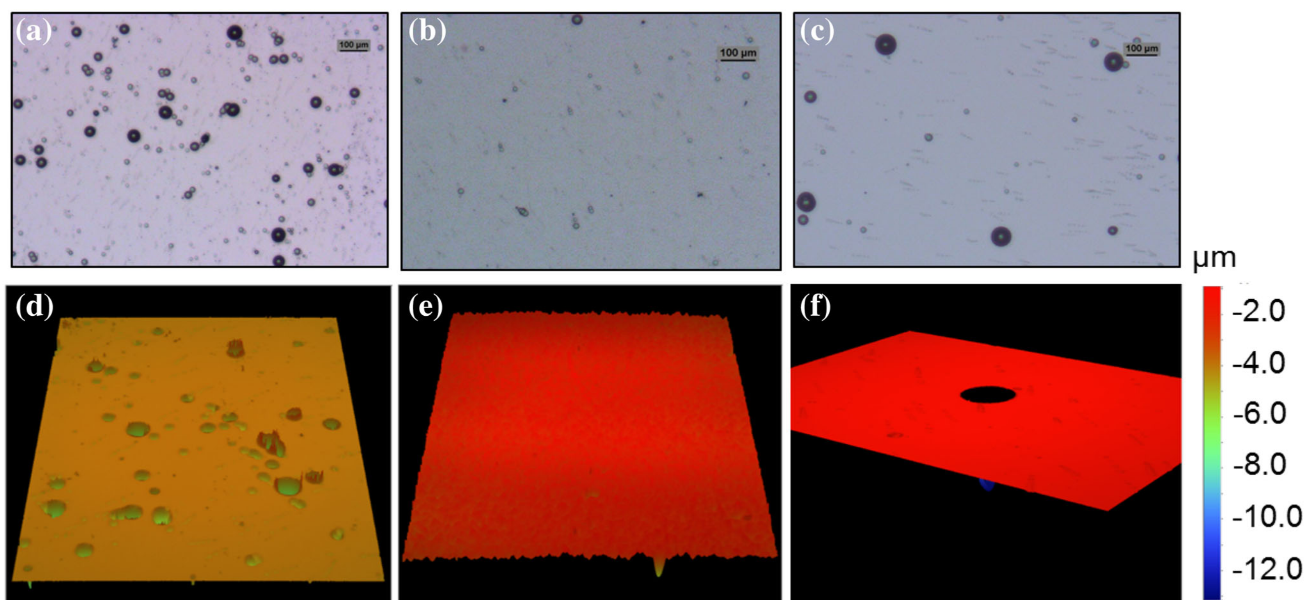

Fig. 10 Optical micrographs (**a–c**) and profilometric images (**d–f**) of the SiC substrates with 8 sccm, 10 sccm and 12 sccm of O_2, respectively, showing the surface morphology after blanket etching

Table 2 Role of O_2 in ICP-RIE etching of SiC

Parameters	Sample # 1	Sample # 2	Sample # 3
Flow rate of O_2 (sccm)	8	10	12
Etch Rate (µm/min)	~ 0.60	~ 0.52	~ 0.58
Average Roughness(nm)	~ 42	~ 17	~ 47

Results and discussion

In the etching process of SiC using ICP-RIE, we have mainly focussed on the ratio of SF_6 and O_2 flow rates in addition to the other process parameters mentioned in the preceding section for optimization of SiC dry-etching. The influence of SF_6/O_2 ratio was studied extensively by varying the flow rate of O_2. During blanket etching, it was observed that a small change in O_2 flow rate changes the surface morphology significantly, which can be observed in optical micrographs and surface profilometry, as shown in Fig. 10. It is quite clear from the figure that O_2 flow rate of 8 sccm provides a rough surface with a high density of etch pits, whereas 12 sccm of O_2 flow rate provides fewer but larger etch pits. It is also observed that O_2 flow rate of 10 sccm exhibits better surface morphology in terms of uniformity and surface roughness. The etch rate and average roughness for different ratios of SF_6 and O_2 are presented in Table 2. The etch rate was estimated to be from 0.5 to 0.6 µm/min, leading to the final thickness of the SiC substrate as 195–160 µm. In SF_6/O_2 gas mixture, SF_6 is the dominant etchant, while O_2 is typically added to enhance the active fluorine concentration that would increase the SiC etch rate (Mehregany et al. 1998; Dowling et al. 2017).

The possible reaction mechanisms are:

$$Si + xF \rightarrow SiF_x, \quad x \le 1-4$$

$$C + xF \rightarrow CF_x, \quad x \le 1-2$$

$$C + nO \rightarrow CO_n, \quad n \le 1-2$$

Oxygen atoms react chemically with carbon atoms in SiC and enhance the etch rates (8 sccm). A higher value of O_2 causes the dilution of reactive particles (fluorine atoms) and produces SiO_x passivation on the surface resulting in a decrease in the etch rate (10 sccm). Further increase of O_2 (12 sccm) creates more volatile products CO, CO_2, etc., and improves etch rates. However, higher O_2% also increases surface roughness, which is not preferable. The optimized flow rates of O_2 and SF_6 were 10 sccm and 50 sccm, respectively, in order to obtain high etch rate and smooth surface morphology with average roughness ~ 17 nm.

Following thinning down the SiC substrate by blanket etching, selective SiC etching was performed using Ni mask to realize the diaphragm structure. This process

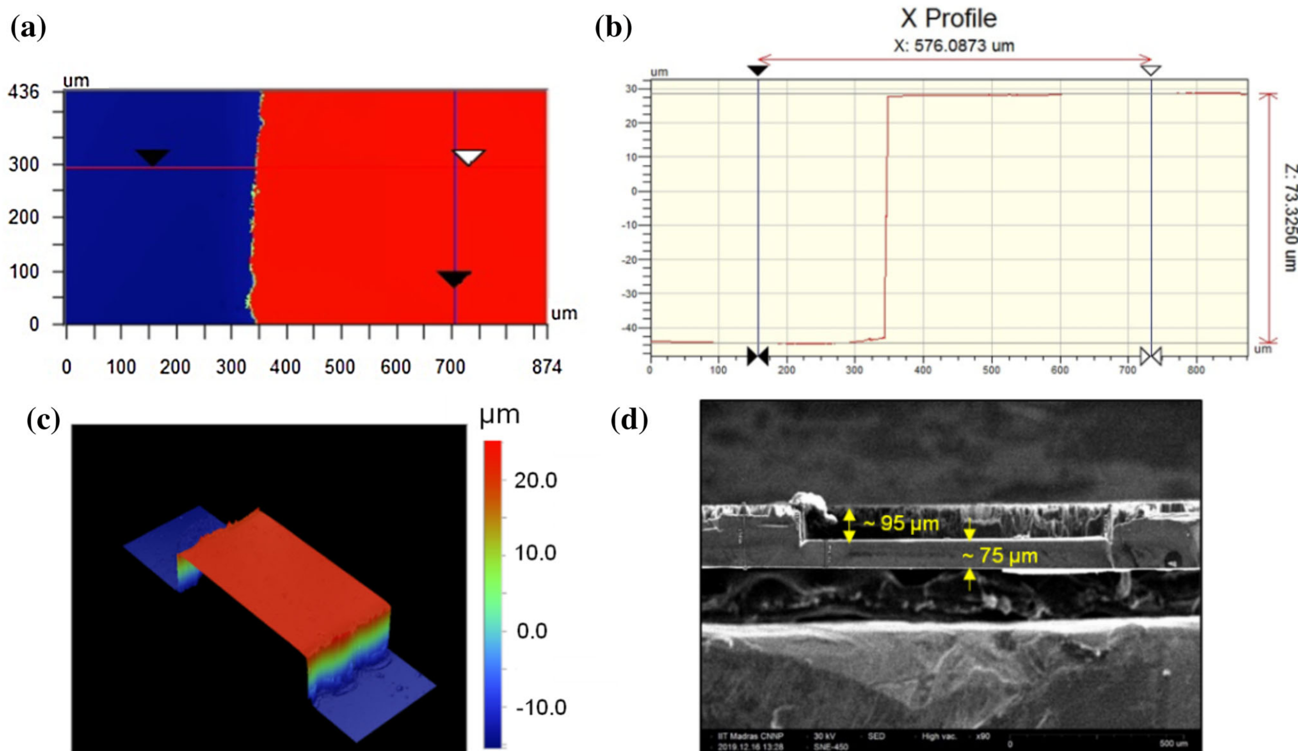

Fig. 11 Etch depth profile (**a**–**c**) and cross-sectional SEM image (**d**) after selective etching of SiC using Ni as mask

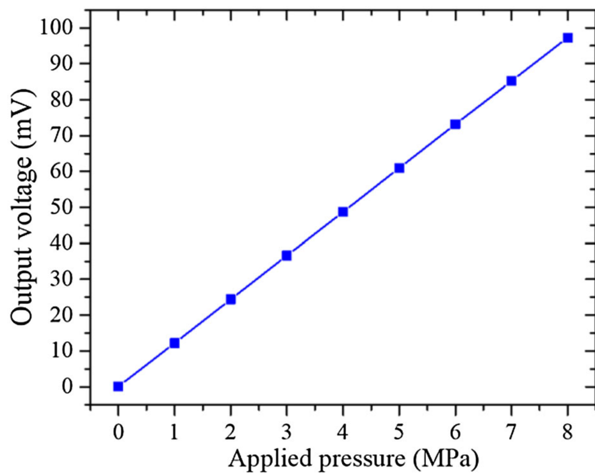

Fig. 12 Response curve between external pressure and output voltage

involves two major parts: (a) deposition of Ni by electroplating using Cr/Au as a seed layer and (b) plasma etching of unmasked SiC. The quality of electroplated Ni plays a major role in selective etching. Peeling off the electroplated metal mask is one of the major problems faced during selective RIE etching of SiC. In order to enhance the adhesion of the seed layer, SiC substrates were heated at 150 °C prior to seed layer (Cr/Au) deposition and the seed layers were deposited at elevated substrate temperature (80 °C). The etch depth profile of SiC after selective etching process was measured using a surface profiler, as shown in Fig. 11a–c. An etch depth of 72 µm corresponds to a SiC diaphragm thickness of 120 µm. With further optimization of the metal mask, an etch depth of 95 µm and SiC diaphragm of 75 µm thickness were achieved, as shown in the cross-sectional SEM image (Fig. 11d). The selectivity of Ni mask over SiC is found to be 10–12.

In post-virtual fabrication scenario, 4H–SiC MEMS pressure sensor is simulated for pressure ranging from 0 to 8 MPa and the corresponding change in the output voltage was observed. The bridge supply voltage was + 5 V_{dc}. The response curve for pressure sensors is shown in Fig. 12. As the pressure difference across the diaphragm increases, the output voltage also increases linearly. According to simulation results, a high value of sensitivity of the pressure sensor is obtained at 2.42 µV/V/KPa. The results obtained from the device simulation software show good linear behavior with respect to applied pressure. The comparative analysis of the virtually fabricated sensor with other reported works is given in Table 3.

Conclusion

In the present study, a complete design, FEM simulation, analysis and virtual fabrication methodology is carried out for the realization of 4H-SiC MEMS pressure sensor using type SiC epitaxial piezoresistors on HPSI SiC substrate. SiC is suitable to realize the sensors for harsh environments. The sensor design, simulation and analysis of the thin square SiC diaphragm and *p*-type SiC resistors are successfully performed using device simulation software for measuring the pressure in 0–8 MPa range. The 4H–SiC MEMS pressure sensor is fabricated using MEMS technology. The sensitivity 2.42 µV/V/KPa (full-scale output) for the pressure sensor is obtained. Comparative analysis suggests that the unique combination of the pressure sensor can be fabricated on the *p*-type epitaxial HPSI SiC Substrate. Based on the primary design, micromachining of SiC diaphragm was performed using ICP-RIE. Both blanket etching and selective etching of SiC using Ni as metal mask were adopted to fabricate the SiC diaphragm. ICP-

Table 3 Comparative analysis of SiC MEMS pressure sensor (NA: Not Available)

Diaphragm material	SiC resistor	Diaphragm size (mm)	Diaphragm thickness (µm)	Sensitivity (µV/V/KPa)	Pressure (MPa)	Supply Voltage(V)	References
HPSI–SiC	*p*-type 4H–SiC	1.5 × 1.5	75	2.42	8	5	Present work
HPSI–SiC	*n*-type 4H–SiC	ϕ 1	50	2.5	1.38	10	Okojie et al. (2015)
n-type 4H–SiC	*n*-type 4H–SiC	ϕ 1	50	2.68	6	1	Akiyama et al. (2011)
n-type 6H–SiC	*p*-type 6H–SiC	1.48 mm^2	50	1.18	6.89	5	Okojie et al. (1998)
n-type 6H–SiC	p-type 6H–SiC	NA	NA	3.3 µV/KPa	1.2	1 mA	Wieczorek et al. (2007)

RIE of SiC in $O_2 + SF_6$ was optimized to obtain an etch rate of 0.6 μm/min maintaining uniformity. The ratio of the flow rate of O_2: SF_6 was found to be a crucial parameter for selective SiC etching by ICP-RIE. Finally, SiC diaphragm of thickness 75 μm was obtained by optimizing Ni electroplating and SiC etching without peeling off the metal mask.

Acknowledgements Authors would like to thank all the scientific and technical staff of Electronics & Instrumentation Group, Material Science Group of IGCAR and IITM, Chennai. The authors also would like thank to Dr. Santanu Parida, MSG, IGCAR for preparation of the paper.

References

Akiyama T, Briand D, Rooij NF (2011) Piezoresistive n-type 4H–SiC pressure sensor with membrane formed by mechanical milling. Proc IEEE Sens 222–225

Barlian AA, Park W-T, Mallon JR, Rasteger AJ, Beth LP (2009) Review: semiconductor piezoresistance for microsystems. IEEE Conf Proc 97(3):513–552

Dowling KM, Ransom EH, Senesky DG (2017) Profile evolution of high aspect ratio silicon sarbide trenches by inductive coupled plasma etching. J Microelectromech Syst 26:135–142

Eickhoffa M, Mollera H, Kroetza G, Bergb JV, et al (1999) A high temperature pressure sensor prepared by selective deposition of cubic silicon carbide on SOI substrates. Sens Actuators A 74:56–59

Hou SM-C (2003) Design fabrication of MEMS-array pressure sensor system for passive underwater navigation inspired by the lateral lines. Dissertation, Massachusetts Institute of Technology

Hsu T-R (2008) MEMS and microsystems: design manufacture and nanoscale engineering. Wiley

Lebedev AA, Ivanov AM, Strokan NB (2004) Radiation resistance of SiC and nuclear-radiation detectors based on SiC films. Semiconductors 38(2):125–147

Mario DG (1982) Flat and corrugated diaphragm design handbook. CRC Press

Mehregany M, Zorman CA, Razan N, Wu CH (1998) Silicon Carbide MEMS for harsh environments. IEEE Conf Proc 86(8):1594-1609

NajafiSohi A (2013) A multifunctional MEMS pressure and temperature sensor for harsh environment application. Dissertation, University of Waterloo

Nguyen T-K, Phan H-P, DinhToan TT, Nakamura K, Foisal ARM, Nguyen N-T, Dao DV (2018) Isotropic piezoresistance of p-type 4H–SiC in (0001) plane. Appl Phys Lett 113:012104

Okojie RS, Ned AA, Kurtz AD (1998) Operation of α (6H)-SiC pressure sensor at 500°C. Sens Actuators A 66:200–204

Okojie RS, Lukco D, Nguyen V, Savrun E (2015) 4H–SiC piezoresistive pressure sensors at 800°C with observed sensitivity recovery. IEEE Electron Device Lett 36(2):174–176

Sawhney AK (1995) Electrical & electronics measurement and instrumentation. Dhanpat Rai & Sons New Delhi

Shore JS, Goldstein D, Kurtz AD (1993) Characterization of *n*-type *β*-SiC as a piezoresistor. IEEE Trans Electron Devices 40(6):1093–1099

Tanaka S, Rajanna K, Abe T, Eshashi M (2001) Deep reactive ion etching of silicon carbide. J Vac Sci Tech B 19(6):2173–2176

Wieczorek G, Schellin B, Obermeier E, Fagnani G, Drera L (2007) SiC based pressure sensor for high-temperature environments. IEEE Sensors Conf Proc 748–751

Wijesundara MBJ, Azevedo RG (2011) Silicon carbide microsystems for harsh environments. Springer, London

Wu C-H, Stefanescu S, Kuo H-I, Zorman CA, Mehregany M (2001) Fabrication and testing of single crystalline 3C–SiC piezoresistive pressure sensors. Transducers' 01 Eurosensors XV Springer

Zappe S, Franklin J, Obermeier E, Eickhoff M, Moller KG, Rougeot C, Lefort O, Stoemens J (2001) High temperature 10 bar pressure sensor based on 3C-SiC/SOI for turbine control applications. Mater Sci Forum 353–356:753–756

Zettterling C-M (2002) Process technology for silicon carbide devices. INSPEC: UK

Publisher's Note Springer Nature remains neutral with regard to jurisdictional claims in published maps and institutional affiliations.